UDC 533.9

# VUV RADIATION DURING PLASMA/SURFACE INTERACTION UNDER PLASMA STREAM POWER DENSITY OF 20 ÷ 40 MW/CM²


***S.G. Vasenin[1], N.I. Arkhipov[1], V.P. Bakhtin[1], S.M. Kurkin[1], V.M. Safronov[1], D.A. Toporkov[1], H. Wuerz[2], A.M. Zhitlukhin[1]***

***[1] Troitsk Institute for Innovation and Fusion Research, 142190 Troitsk Russia***

***[2] Forschungszentrum Karlsruhe, P.O. Box 3640, 76021 Karlsruhe Germany***


## 1. Introduction

An interest in powerful hydrogen plasma gun application for solid-state materials treatment has increased in the past few decades. Current powerful plasma guns – MK-200, QSPA, MKT (TRINITI, Russia), QSPA Kh-50 (KIPT, Ukraine), VIKA (Efremov Institute, Russia), PLADIS (USA) – are employed widely both for plasma/surface interaction investigation [1-5] and for surface modification [6].

With the onset of action of powerful plasma stream an exposed surface begins being quickly eroded. As a result, dense plasma containing target ions forms near the target surface. In several μs impacting hydrogen ions cannot reach the surface directly and further energy transfer to the surface is determined by transport in target plasma. Electron density profile increasing as the surface is approached makes radiant heat transfer onto the surface difficult. Only a small part of hydrogen stream energy can attain the target surface. The rest of the stream energy can be accommodated by three possible ways: 1) hydrogen ions conserve their energy and don't transmit it to target ions; 2) hydrogen ions do transmit energy to target plasma that can flow around an exposed target; 3) there is effective energy transmission to target plasma which, in its turn, re-radiates the bulk of transmitted energy into the surroundings. First case is common to experiments where fairly dense and rather cold hydrogen plasma is used, and so self-retarding of hydrogen plasma takes place. Second case is characteristic for plasma/surface interaction without strong longitudinal magnetic field, which would prevent plasma from transversal motion and so, in the first place, would prevent hydrogen plasma from flowing around the target and, secondly, would prevent target plasma from mass loss due to its transverse motion. In respect to radiative properties of target plasma the third case is the most attractive. High directed velocity accompanied with moderate density of hydrogen stream is favorable for energy exchange with target plasma, and strong magnetic field prevents target plasma from transversal spreading and assists in plasma heating. An efficiency of stream energy conversion into VUV radiation is expected to be maximal in this case. It is these conditions of plasma/surface interaction that have been realized at MK-200UG plasma facility. Extensive set of VUV radiation diagnostic techniques – 2D radiating region mapping, time-integrated and time-resolved VUV spectroscopy, radiation calorimetry – along with tools for plasma stream properties measurements make possible analysing the role of VUV radiation at plasma/surface interaction process.

## 2. Experimental facility and diagnostic techniques

The experiments were performed at the MK-200UG facility (Fig.1). It consists of MK-500 pulsed plasma gun, 9.5-m length drift tube filled with a longitudinal magnetic field and a target chamber with attached diagnostic tools. The drift tube consists of cylindrical and conical sections. The magnetic field strength is about 0.7 T in a cylindrical part and it rises from 0.7 T up to 2 T along a conical part.

The plasma gun injects a supersonic hydrogen plasma stream into the drift tube. While a plasma stream moves in the long drift tube, its length increases because of plasma velocity dispersion. Passing through increasing magnetic field a supersonic plasma stream is compressed in radial direction and is effectively magnetised.

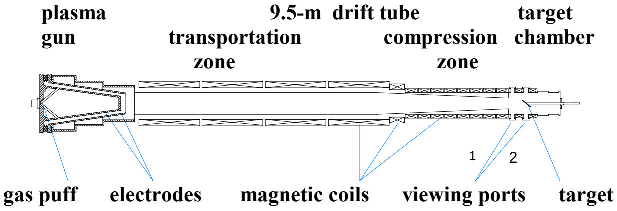


*Fig.1. Principal scheme of MK-200UG facility*

Interaction with a target occurs in a target chamber 30-cm in diameter and 50-cm in length. There is a longitudinal magnetic field of 2 T in the chamber. Parameters of free plasma stream at a target position are the following: energy density q≈ 1.2 kJ/cm²; power density W = 20 ÷ 40 MW/cm²; plasma stream duration τ≈ 40 μs; directed ion energy $E_i$= 1.5 keV (it decreases down to 300 eV by the end of the pulse); electron density n = (2 ÷ 6)×$10^{15}$ $cm^{-3}$; electron temperature $T_e$= 200 ÷ 100 eV; beta value $\beta = 8\cdot\pi\cdot P/B^2$ =0.3; effective plasma stream diameter D ≈ 7 cm. The plasma stream parameters are practically constant along the target chamber length. An exposed target has been installed in the chamber normally to impinging plasma stream.

High-sensitive thermoelectric radiation calorimeter [7] is employed for time- and spectrum integrated measurements of radiative loss from target plasma. Aluminium oxide film is used as a facing coating. It provides an absorption coefficient K being more than 98% for spectral band 4 A<λ <12 μm, with the exception of region 240 A <λ< 2400 A where K ≥ 85% [7].

2D maps of radiating plasma region distribution are taken with a help of pinhole camera. A 4x2 pinhole array forms 8 images on input face of circular microchanel plate (MCP) [8]. The input face has been electrically divided into 8 pieces. The pieces are fed one after another by their 100-ns gating pulse. As a result 8 frames with 100-ns exposure are captured. All electron images are converted into visible ones via a phosphor and then they fiber-optically make a replica on Kodak 2484 film. No filter has been used and so the region λ< 1500 ÷ 2000 A, defined only by MCP spectral sensitivity, is under study.

To perform VUV spectral measurements a transmission grating spectrometer has been chosen. An employed free-standing gold grating has period of 2000A. Time-integrated spectra have been recorded with XTE/CCD-1024 TKB/1 back-illuminated CCD camera [9] or Kodak 101 X-ray film. MCP-based multiframing camera [8] has been used for taking 4 time-resolved spectra with 100-ns exposure duration.

## 3. Experimental results

Pinhole frames of plasma radiation demonstrate that strong magnetic field suppresses effectively a transversal motion of target plasma. As a result of quasi-1D motion of radiating ions, an emitting plasma column, which is extended along magnetic field lines and which has rather sharp edges, appears in front of exposed target. For example, Fig.2 displays pinhole pictures near tungsten target 5-cm wide. An appearance of emitting region, its growth and a formation of stable plasma column are clearly seen in successive frames. It should be mentioned that radiating column is slightly wider than the target width (6 ÷ 7 cm vs. 5 cm) and its width doesn't alter with a distance from the target surface.

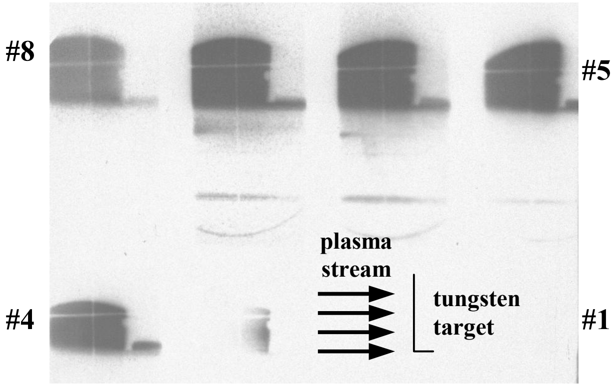


*Fig.2. Pinhole frames of tungsten plasma radiation at λ< 1500 ÷ 2000 A. Interval between next frames – 2 μs*

Radiative loss measurements have been performed for two targets: first one is of tungsten of size L×H×δ =10.6×3.4×0.3 cm and second one being of graphite with size L×H×δ = 14×4×1 cm. To evaluate optical thickness of plasma the measurements have been carried out with vertical and horizontal orientation of a target. Horizontal orientation means that a target is viewed by calorimeter along short side (H=3.4 cm – for tungsten; H=4 cm – for graphite); vertical orientation – along long side. Horizontal orientation is standard one. In this case peripheral regions of emitting plasma column – that have radiative properties different from central region's ones – are out of calorimeter sight. We'll use results of measurements with vertical orientation for rough estimation of optical thickness of radiating column only. Actually, if plasma is optically thick, plasma column emittance doesn't depend on column length along view axis. If plasma is optically thin, then plasma emittance is proportional to plasma length. In other terms: $B_{horiz}/B_{vertical} \approx 1$ - for optically thick plasma; $B_{horiz}/B_{vertical} \approx H/D \approx 1/2$ - for optically thin plasma.

Results of calorimetric measurements for tungsten and graphite are shown in Fig.3 and 4 respectively.

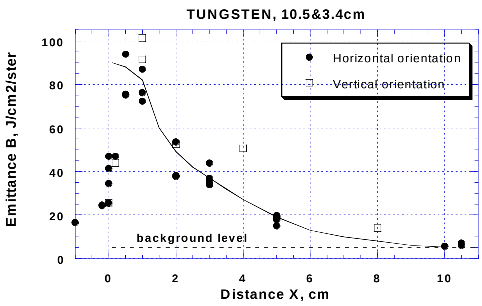


*Fig.3. Plasma column emittance spatial distribution along a distance from tungsten target*

For tungsten target an emittance profile is sharply peaked close to the surface. Taking into account that background level is $B_0$ = 5 J/(cm$^2$·ster), one may conclude that the profile half-width is ΔX= 1.5 cm and maximal magnitude is $(B - B_0)$ = 85 J/(cm$^2$·ster) at X≈0. In space region X > 8 cm radiation is practically absent. From analysis both target orientation a conclusion can be drawn that at a distance X < 2 cm plasma layer is optically thick and at a distance X > 2 cm it is optically thin. Notice that such an estimation of optical thickness doesn't relate to each spectral region, but to whole spectrum only, or, in other words, it is effective optical thickness.

Emittance profile for graphite plasma proves to have a similar shape – maximum is near surface, emittance decreases with a distance as well. But the rate of fall is much less. One can see that at a distance X < 8 cm there is a large scatter in data. Nevertheless, almost all experimental points lie closely along two curves. It prompts to the conclusion that there are two different regimes of plasma column emission: type 1 (lower curve) and type 2 (upper curve). It seems reasonable to assume that type 1 and type 2 distinct from each other according to high Z impurities. Type 1 seems to correspond to "rather clear" plasma in plasma column. Type 2 is likely to match a shot when plasma column contains impurity ions. Scenario for impurity appearance could be the following. In a certain shot, plasma stream touches conical part of drift tube of stainless steel. It results in vaporisation of some mass of high Z materials (iron, nickel, etc.) and subsequent vapour deposition on exposed surface of a target. In subsequent shots high Z ions give significant contribution into plasma column emittance if a target is made of low Z materials, for example, of graphite. It will continue until a target surface is gradually cleaned by plasma exposure. Since this moment till next touch only radiation of target plasma itself will be visible.

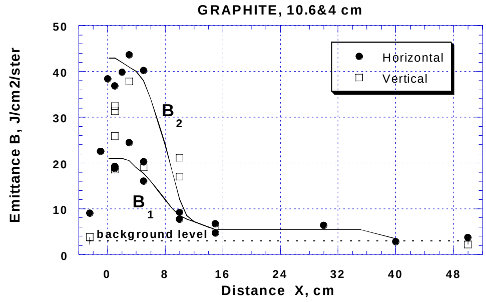


*Fig.4. Plasma column emittance spatial distribution along a distance from graphite target*

In a "pure" regime a peak of emittance is $(B - B_0) \approx 18$ J/(cm$^2$·ster), in second regime it is $(B - B_0) \approx 40$ J/(cm$^2$·ster). Curves for both regimes have half-width of ΔX= 8 cm. At a distance X > 10 cm the curves coincide. This peculiarity is consistent well with suggested interpretation of experimental data. Comparing two target orientations one can conclude that plasma column is optically thick for X < 5 cm and optically thin for X > 10 cm. At a distance X> 10 cm plasma column is likely to consist of carbon and hydrogen plasmas only. In wide spatial region 15 cm < X < 35 cm plasma column emittance remains practically unaltered $(B - B_0) \approx 2 \div 3$ J/(cm$^2$·ster). An emittance obtained at a distance X> 40 cm is not quite correct, because for these measurements a target has to be positioned into region of magnetic field attenuation

Using emittance data and optical thickness estimations one can calculate specific radiative loss of plasma column (i.e. loss per column cross section unit). For tungsten it proves to be of 0.9 ÷ 1 kJ/cm$^2$. It means that an efficiency of plasma stream energy transformation into VUV radiation is about unity. For graphite target relevant radiative loss are of 0.6 ÷ 0.7 kJ/cm$^2$ for "pure" regime and of 1 ÷ 1.1 kJ/cm$^2$ for another regime. These values are obtained by integrating over X from zero to 40 cm, i.e. over the range where reliable data on plasma emittance exist. Hence an efficiency of energy conversion is rather large (50% ÷ 90%) for graphite as well.

Spectral measurements indicate that plasma near graphite target consist mainly of carbon ions $C^{4+}$, $C^{5+}$ (and perhaps $C^{6+}$). Resonant lines CV 40.3A ($1s^2$-1s2p) и CVI 33.7A (1s-2p) are dominant in a spectrum. This peculiarity is most pronounced at a large distance from a target (see, for instance, Fig.5 for X=38 cm). The $C^{4+}$ ion line is prevalent at a distance X< 5; the $C^{5+}$ ion line is dominating at a distance X> 5 cm (Fig.6). There is no evidence of $C^{3+}$ ion lines existence even in the vicinity of the graphite target. Along with characteristic narrow distinct lines of carbon ions a considerable radiation at wavelength 165 ÷ 220A are clearly seen in some spectra detected. This radiation is likely to belong to iron ions Fe IIV – Fe IX lines and it is apt to correspond to second regime of plasma column emission. The fact that a peak of radiation is situated close to target surface (see Fig.6) proves the assumption.

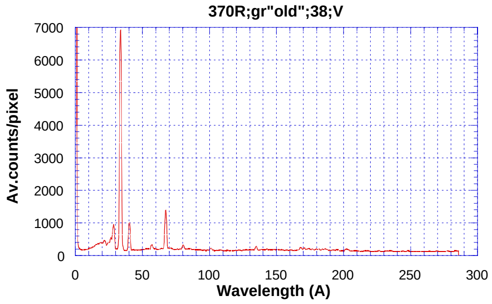

*Fig.5.Time-integrated spectrum at a distance of X=38 cm from graphite target*

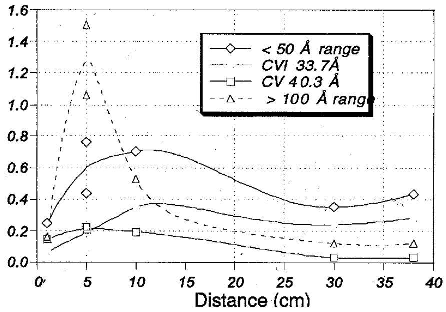

*Fig.6. Spatial distribution of plasma column radiance (in relative units) vs. the distance from graphite target*

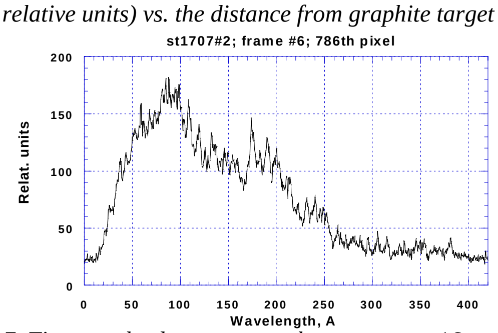

*Fig.7. Time-resolved spectrum at the moment τ≈ 16 μs at a distance of X=2 cm from tungsten target*

A spectrum of tungsten plasma at a distance X= 2 cm is presented in Fig.7. It is time-resolved spectrum corresponding to the moment τ≈ 16 μs from interaction onset. As distinct from graphite plasma, high Z ions of tungsten emit radiation in wide spectral band 30 ÷ 300A. The spectrum looks like quasi-continuum and has two smooth maximums: around 90A and around 190A. Region around 90A is prevailing. It should be pointed out that at time-integrated spectral measurements at the same distance or at time-resolved measurements at late moments another spectral region – 160 ÷ 260A – dominates over a spectrum. This characteristic feature of tungsten spectra can be explained taking into account that at electron temperatures 20 ÷ 50 eV, that are typical for plasma column [10], a mean charge of tungsten ions changes from 10 to 17 [11]. As a consequence even small variation in plasma temperature can lead to change in prevailing ion charge and it can be accompanied by a transformation of emitted spectra.

Pinhole pictures and time-resolved spectra reveal the fact that duration of intense VUV emission of target plasma is about 25 μs what is considerable less than hydrogen stream duration (about 40 μs). It takes place both for graphite and for tungsten target, and so it cannot be accounted for by particular features of space distribution of intense re-radiating regions. Observed fall of plasma emission seems to result from a drop of electron temperature of target plasma owing to decreasing of rate of energy flux being transmitted from hydrogen stream to target plasma. By the moment τ≈ 25 μs the boundary separating retarded part of hydrogen stream from moving tail part of the stream seems to move away from a target surface at a distance, which is large enough for making difficulties for energy transport from tail part to target plasma. It takes place even for a case of graphite plasma when a target plasma leading edge recedes from a target surface as well [12].

According to an estimation, by the moment τ = 25 μs a tail part of plasma stream carries one-third of total stream energy. The termination of intense VUV emission is indicative of a drop of energy afflux into target plasma. It means that one-third of stream energy cannot be transformed into VUV radiation energy. Nevertheless, it seems to be quite reasonable to talk of high – up to unity – efficiency of energy conversion into VUV radiation. The point is that total plasma stream energy is not a convenient quantity to be manipulated with.

Plasma stream energy is measured with calorimeter. It is well known [13] that proper choice of calorimeter material and its sizes provides almost net energy absorption of plasma entering calorimeter. But there is no reliable evidence that calorimeter can appropriately measure an energy of tail part of plasma stream. (Measurements of moderate density plasma stream flowing in strong magnetic field are meant here. Only measurements of the kind are possible at MK-200UG, because strong magnetic field is necessary for successful plasma transportation at the facility.) It is quite reasonable to consider that calorimeter gives underestimated magnitude of total plasma stream energy. In a more general way, any use of plasma stream energy must be accompanied by its slowing-down. Under certain circumstances – when plasma motion is quasi-1D and plasma density is not very low – plasma stream self-retarding takes place and energy of tail part is delivered into region of its use by electron heat conductivity. Decreasing of electron temperature and ion directed energy along a length of plasma flow is intrinsic to plasma stream generated by plasma gun. Because heat conductivity changes abruptly with electron temperature variation, only a portion of tail part energy can be delivered into region of its use. For this reason it would be prudent to measure plasma stream energy on the basis of data from calorimeter. We followed this approach throughout this paper. It hardly tends to be confusing when kept in mind that an expression "stream energy" stands for usable part of its energy.

## 4. Conclusion

Properties of VUV radiation resulting from interaction of powerful high-temperature hydrogen plasma stream with target of tungsten and of graphite have been investigated at MK-200UG plasma facility. Dramatic distinction between spectra of graphite and tungsten plasma has been discovered. But in both cases VUV radiation plays an important part in energy balance of plasma/surface interaction. VUV emission duration proves to be noticeably less than plasma stream duration. This fact can be construed on the basis of considering energy transfer from hydrogen plasma stream to target plasma.

This work was supported in part by MINATOM RF under contract no. 6.23.19.19.00.924 and by the Russian Foundation for Basic Research (project no. 00-02-18028).

## References

1.H. Wuerz et al., Fusion Technology, vol.32, no.1, 1997, p.45
2.V. Belanp et al., J. Nucl. Mater., 241 – 243, 1996, p.763.
3.V. Chebotarev et al., J. Nucl. Mater., 233 – 237, 1997, p.736
4.V. Kozhevin et al., Fusion Eng. Des., 28, 1993, p.157
5.J. Crawford et al., J. Nucl. Mater., 203, 1993, p.280
6.B. Kalin et al., Surface and Coatings Techn., 96, 1997, p.110
7.B. Bruntkin at al., Techniques for studying spectral and relaxation properties of atoms and ions, M., 1990 (in Russian)
8.D. Toporkov et al., Instruments and Experimental Techniques, vol.41, no.1, 1998, p.114
9.N. Arkhipov et al., J. Nucl. Mater., 266 – 269, 1999, p.751
10.N. Arkhipov et al., Plasma Phys. Rep., vol.24, 1998, p.340
11.H. Wuerz et al., Report FZKA 6198, 1999
12.N. Arkhipov et al., Plasma Phys. Rep., vol.25, 1999, p.236
13.N. Arkhipov et al., 3rd All-Union Conference on Hot Plasma Diagnostics, Dubna, 1983, p.98 (in Russian)